# Galactic Nuclei in the Cosmological context 2024


https://gnc2024.physics.muni.cz/

# “Housekeeping” rules

- each speaker has 30 **minutes** that should roughly consist of 25 min talk and 5 min discussion
- after the meeting, I will ask for **pdf files** of your presentations and put them on the website (accessible also via **NASA ADS**)
- please select your lunch menu for Tuesday and Thursday
- please indicate if you are joining for the trip to Świnoujście (on Wednesday), we will clarify the pick-up spot on Tuesday
- on Monday (Welcome Drink & Dinner from $\sim 19:00$ Nowy Browar) and on Thursday (Morskie Centrum Nauki from $\sim 16:30$)


# Scope of the GNC24 meeting

Galactic nuclei in the cosmological context

**Michal Zajaček**

**N. Khadka, S. Cao, Z. Yu, M. L. Martínez-Aldama, S. Panda, R. Prince, B. Czerny, B. Ratra, M. Naddaf**

Faculty of Science, Masaryk University

**GNC 2024 meeting**

June 3rd, 2024

# Two main directions

## Seeds and growth of supermassive black holes

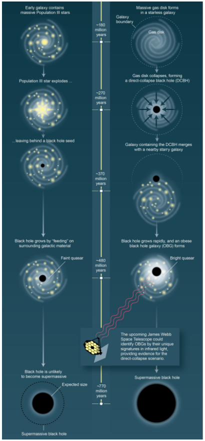


Credit: Natarajan

## Accreting supermassive black holes as cosmology probes

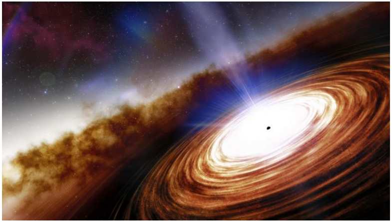

J0313-1806 ($z = 7.64$); Credit: NOIRlab

# Two groups: Quasar group

Led by **Prof. Bozena Czerny** (CFT PAS, EAS Lodewijk Woltjer lecture 2022)

# Two groups: Cosmology group

Led by **Prof. Bharat Ratra** (Kansas State University, AAS Fellow)

# Why to combine active galactic nuclei and cosmology?

- it may seem that we have a good understanding of both
- Active Galactic Nuclei (AGN): standard disk solution (1973): Shakura-Sunyaev, Novikov-Thorne, Blandford-Znajek, Blandford-Payne ...
- standard (concordance, benchmark) $\Lambda$CDM model ($\Lambda$ - cosmological constant proportional to the dark energy density, CDM - cold dark matter) can address hot Big Bang, cosmic microwave background, homogeneous and isotropic Universe on large scales, structure formation on smaller scales ...
- this is mostly an illusion $\rightarrow$

# Current expansion rate of the Universe in trouble

- value determined from nearby (late-Universe) probes is larger than the value inferred from the Cosmic Microwave Background (early-Universe)
- Hubble tension ($H_0$ tension)

**Early Universe**
**z ~ 1000**

Cosmic microwave background (CMB)

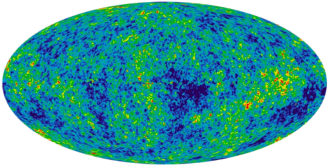

$H_0 = 67.66 \pm 0.42\,\mathrm{km\,s^{-1}\,Mpc^{-1}}$

Plank collaboration 2018

⊢ 4σ ⊣

**Late Universe**
**z <1**

Cephids, SNIa

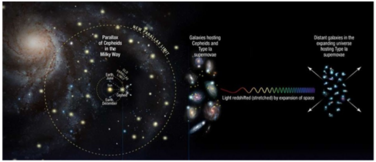


$H_0 = 74.03 \pm 1.42\,\mathrm{km\,s^{-1}\,Mpc^{-1}}$

Riess et al. 2019

# Current expansion rate of the Universe in trouble

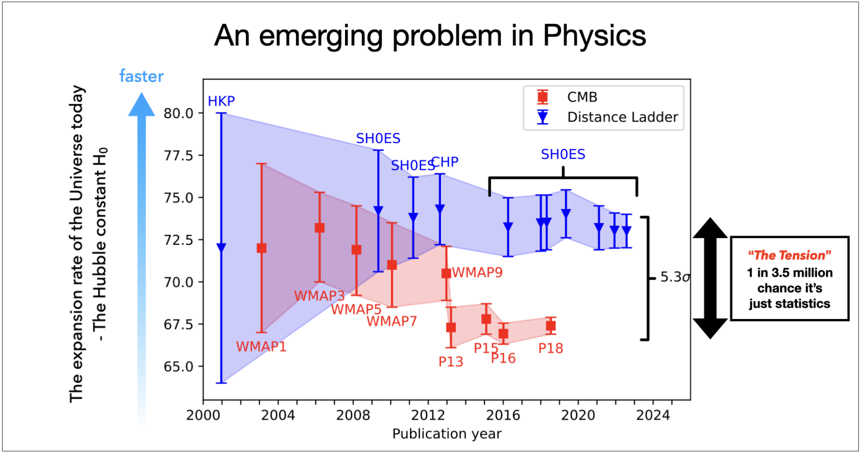


- $H_0$ tension could be caused by **systematic problems in some of the standard cosmological probes** or **it could imply problems with the standard concordance model**

# Search for new probes

- **active galactic nuclei (AGN) or quasars** could provide a **bridge** between early-Universe measurements (CMB, BAO) and late-Universe measurements (SNIa)

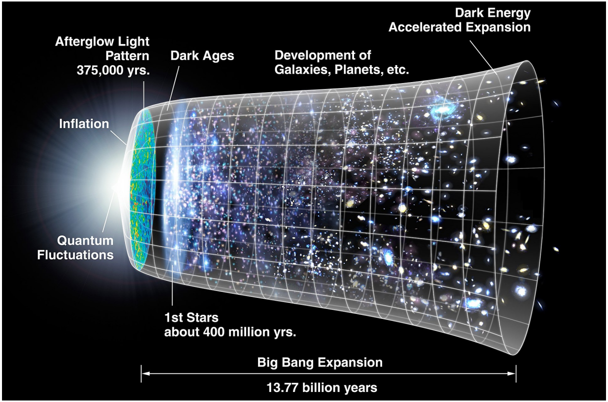

# Discovery of quasars

Optical counterpart of the radio source 3C 273 was identified based on the precise measurements of the Moon occultation of the radio source by the Parkes radio telescope (Cyril Hazard and John Bolton). Based on that, **Maarten Schmidt** could find the optical counterpart and obtain the optical spectrum, which contained “unusual” **broad lines**.

**Schmidt realized that these lines are redshifted hydrogen emission lines, which put 3C 273 at a cosmological redshift of 0.158 (749 Mpc) $\rightarrow$ letter to Nature on March 16, 1963 (almost exact 61st anniversary).**

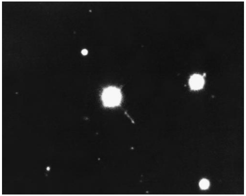

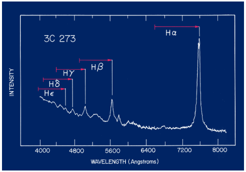


# Towards unification scheme

- not all (active) galactic nuclei have broad lines (Sgr A*)
- some only have narrow components (type 2 sources vs. type 1 with also broad components present)
- a breakthrough discovery came in the study of the total and the polarized optical emission by **Antonucci & Miller (1985)**
- they studied a well-known 'type 2 source' NGC 1068

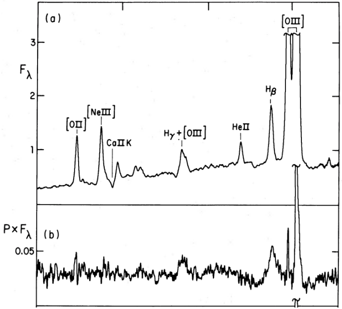

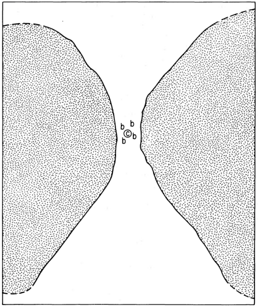

# Unified scheme

Properties of active galactic nuclei (AGN) are mainly determined by viewing angle

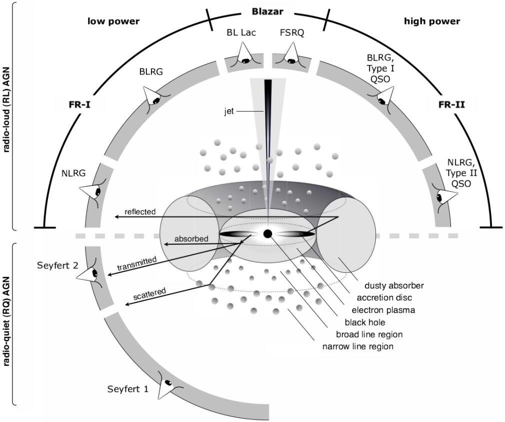


Taken from Beckmann & Schrader (2012)

# Relation between UV and X-ray emission

- There is a significant correlation between UV luminosity ($L_{\rm UV}$) and the X-ray luminosity ($L_{\rm X}$)
- $L_{\rm UV}$ – accretion disc
- $L_{\rm X}$ – hot X-ray corona

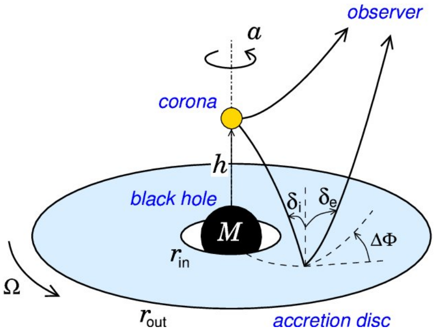


Log-linear relation: $\log L_{\rm X} = \gamma \log L_{\rm UV} + \beta$

# Relation between UV and X-ray emission

- Risaliti & Lusso (2019) applied the relation to derive the luminosity distance $D_{\rm L}$ of quasars, which allowed to construct the **Hubble diagram of quasars**

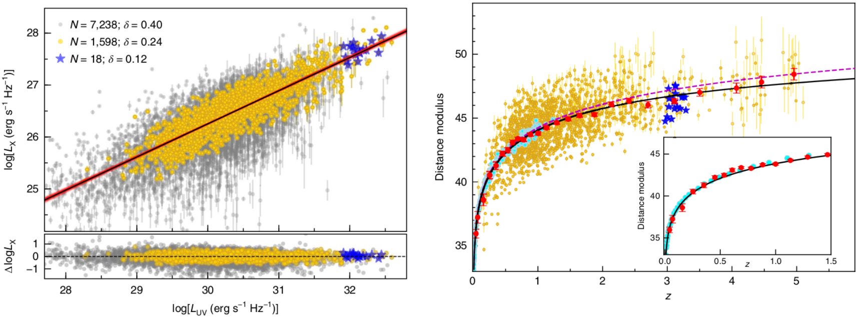

# Relation between UV and X-ray emission

- $D_{\rm L}$-$z$ indicated larger relative matter content $\Omega_{\rm m0}$ and a dynamical dark energy model with $\rm w_0w_aCDM$ with $w < -1.3$ in the EOS of dark energy

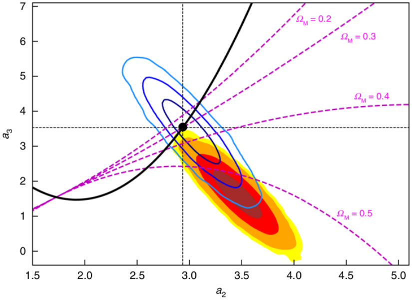


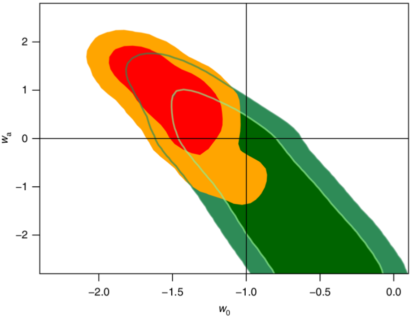


Risaliti & Lusso (2019)

$\rightarrow L_X - L_{UV}$ relation needs to be tested for different cosmological models and as a function of redshift

$\rightarrow$ comparison with another standardization method desired

# Type 1 AGN & Broad lines

- optical domain: H$\alpha$ (656.3 nm), H$\beta$ (486 nm), optical FeII (443.4 nm and 468.4 nm)
- UV domain: MgII (279.8 nm), UV FeII (270-290 nm), CIV (154.9 nm)
- **very broad lines with FWHM**$\geq 2000\,\mathrm{km\,s^{-1}}$ **are the most characteristic features in quasar spectra** (see first works such as Seyfert 1943, Woltjer 1959, Schmidt 1963)

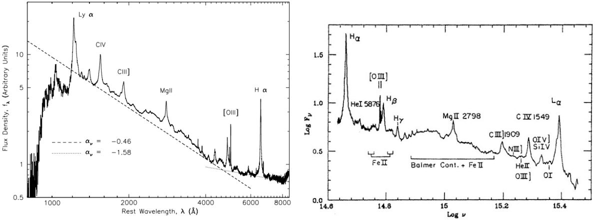


Figure: Left: Composite quasar spectrum in the wavelength domain (Vanden Berk+2001). Right: Composite quasar spectrum in the frequency domain (Courtesy of J. Baldwin).

# BLR: physical model and geometry

- Broad line region revealed by broad lines with FWHMs of several 1000 km/s
- $\rightarrow$ large velocity implies the motion close to the SMBH
- *mean kinematic radius:*

$$r_{\rm BL,kin} = f\frac{GM_{\bullet}}{v_{\rm K}^2} = 0.86f\left(\frac{M_{\bullet}}{2\times 10^8\,M_{\odot}}\right)\left(\frac{v_{\rm K}}{1000\,{\rm km\,s^{-1}}}\right)^{-2}\,{\rm pc}$$
$$\sim 45\,000 f\,R_{\rm s}\,,$$
$$R_{\rm s} = 2GM_{\bullet}/c^2 = 1.9\times 10^{-5}(M_{\bullet}/2\times 10^8\,M_{\odot})\,{\rm pc}$$

- **well inside the Bondi radius and the gravitational influence radius of the SMBH $\rightarrow$ very difficult to resolve spatially**

$$r_{\rm Bondi} \approx \frac{GM_{\bullet}}{c_{\rm s}^2} = 1\,\left(\frac{M_{\bullet}}{2\times 10^8\,M_{\odot}}\right)\left(\frac{T_{\rm g}}{10^8\,{\rm K}}\right)^{-1}\,{\rm pc}\,,$$
$$R_{\rm inf} = \frac{GM_{\bullet}}{\sigma_{\star}^2} \approx 86\left(\frac{M_{\bullet}}{2\times 10^8\,M_{\odot}}\right)\left(\frac{\sigma_{\star}}{100\,{\rm km\,s^{-1}}}\right)^{-2}\,{\rm pc}$$

# BLR: physical model and geometry

- **collection of clouds** (density, temperature) that have a certain geometrical as well as velocity distribution
- move under the influence of the SMBH$+$ radiation pressure from an accretion disk $+$ other effects (gas pressure gradient, magnetic field)
- $\rightarrow$ complex dynamics

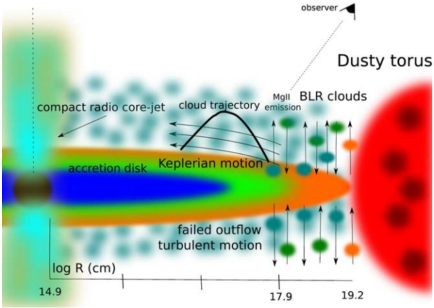


Precise modelling should consider four orders of magnitude in radius.

# BLR: physical model and geometry

- we can distinguish **low-ionization line (LIL)** and **high-ionization line (HIL)** regions
- **HIL** (CIV, HeII, Ly$\alpha$) – higher ionization potential (> 40 eV), less dense clouds, show signs of outflow (line asymmetry, blueshifted line peaks), and are located closer to the SMBH
- **LIL** (H$\alpha$, H$\beta$, MgII, FeII) – lower ionization potential (<20 eV), clouds form closer to or within the disk plane in the denser region, no significant signs of inflow/outflow, dominant Keplerian component

**Collin-Souffrin et al. (1988)**

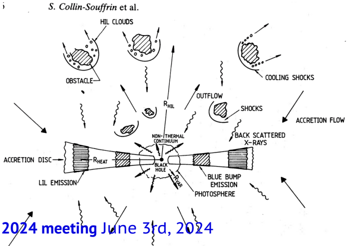

# BLR: LIL clouds

Main properties

(i) from emission properties, it is not quite evident that clouds form a disk-like structure → simple single-peak profiles for Narrow Line Seyfert 1 sources and type A quasars; only some sources have double-peak profiles

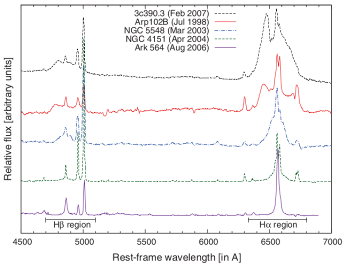


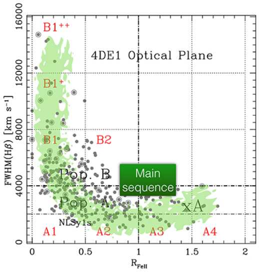


Ilic+2015, Marziani+2018

# BLR: LIL clouds

Main properties

(ii) lines do not indicate strong inflow/outflow (no systematic blueshift or redshift);

(iii) high covering factor ($\sim 30\%$) of the nuclear emission to explain the significant correlation

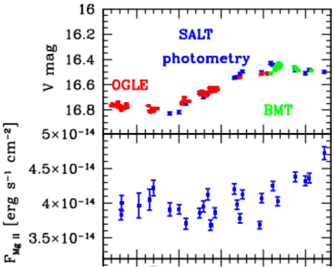


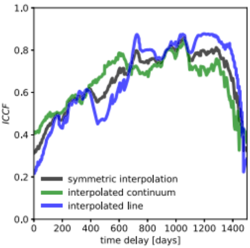


Zajaček+2020 (HE 0413-4031)

# BLR: LIL clouds

Main properties

(iv) absorption is rare, they form a flattened structure following the disk, but not too flat to address the high covering factor (ring-like, torus-like structure). This was recently confirmed by the GRAVITY detection and the phase-resolved observation of Pa$\alpha$ in 3C273

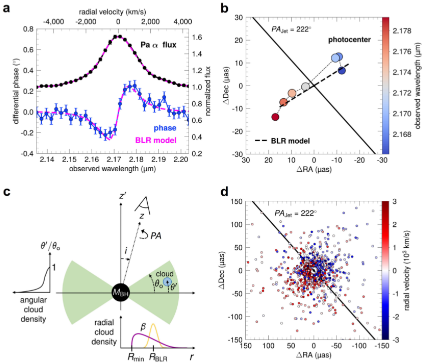

# BLR: LIL clouds

Main properties

(v) need to be dense enough to stay at the temperature of $10 - 20 \times 10^3$ K (similar to HII regions) to emit allowed transitions of the observed strengths.

- one semi-forbidden transition CIII] puts a lower limit on the number density $> 10^9\,\mathrm{cm^{-3}}$
- current photoionization modelling indicates number densities of $n \sim 10^{12}\,\mathrm{cm^{-3}}$, length-scales of $10^{12}\,\mathrm{cm}$ ($\sim 0.07\,\mathrm{AU} \sim 14.4\,R_{\odot}$), which results in the column density of $N \sim 10^{24}\,\mathrm{cm^{-2}}$
- the mass is equivalent to $M_{\rm BLR} \sim \frac{4}{3}\pi R^3 \mu n m_{\rm H} \sim 3.5 \times 10^{24}\,\mathrm{g} \sim 4 M_{\rm Ceres}$ (one cloud has the mass comparable to the whole Main Asteroid Belt)

# BLR: LIL clouds

BLR scales are comparable to the outer Solar system, hence it is difficult to probe directly

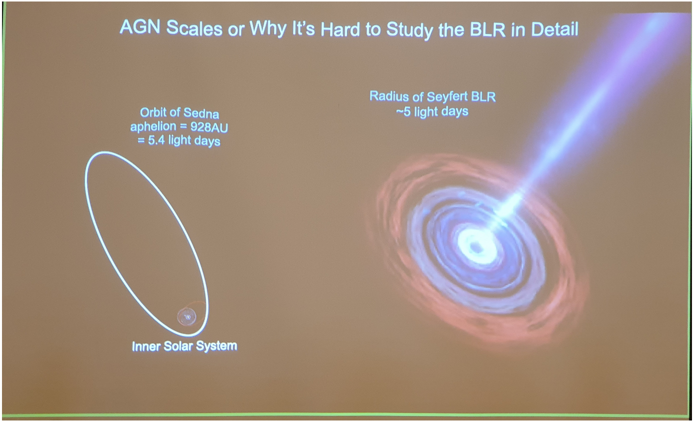


Figure: Courtesy of Misty Bentz

# Reverberation mapping of galactic nuclei

Different wavelengths probe different scales of an accretion flow

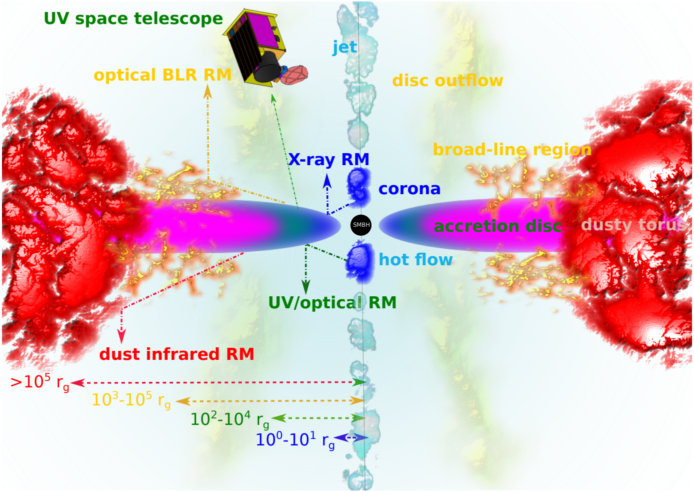

# Reverberation mapping of galactic nuclei – results

- **mean radius of the BLR**: $R_{\rm BLR} \sim c\tau_{\rm rest}$
- the **virial mass of the SMBH**: $M_{\rm vir} = \frac{f_{\rm vir} c\tau_{\rm rest} \mathrm{FWHM}^2}{G}$
- **radius-luminosity relation:** $R_{\rm BLR} = CL_{\rm mon}^{\gamma} \rightarrow$ $log(\tau/\mathrm{days}) = \beta + \gamma \log\left(L_{\rm mon}/10^{44}\,\mathrm{erg\,s^{-1}}\right)$

The power-law slope is expected to be close to 0.5.
This follows from simple photoionization theory of a BLR cloud:

$$U = \frac{Q_{\rm ion}(H)}{4\pi R^2 c n_{\rm e}}\,, Q_{\rm ion}(H) = \int_{\nu_i}^{+\propto} \frac{L_\nu}{h\nu}\mathrm{d}\nu$$

Under the assumption $Un_{\rm e}$ $\sim$konst. for different sources, we can derive $R \propto L^{1/2}$

# H$\beta$ Radius-luminosity relation (low-redshift sources)

Historically, H$\beta$ broad line was used to obtain time delays for lower-redshift sources ($0.0023 \leq z \leq 0.89$).
Earlier data had a small scatter, later the scatter increased due to the presence higher-Eddington sources.

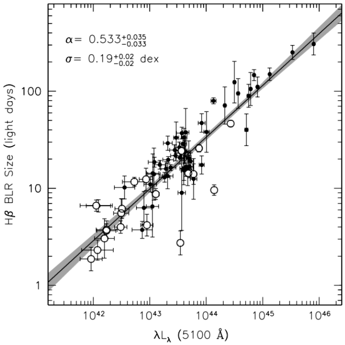


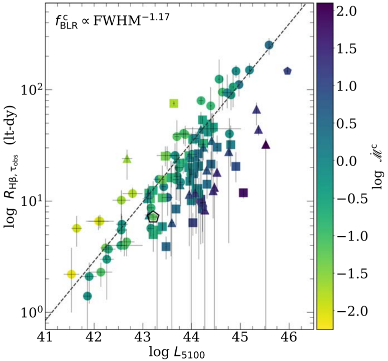


Bentz+13 (71 sources) and Martinez-Aldama+2019 (117 sources)

# MgII Radius-luminosity relation (intermediate-redshift sources)

Czerny+2019, Zajaček+2020, and Zajaček+2021 construct first MgII radius-luminosity relations for higher-redshift sources in the range $0.0033 \leq z \leq 1.89$ (10, 11, and 69 measurements). Current source number is **194!!!**

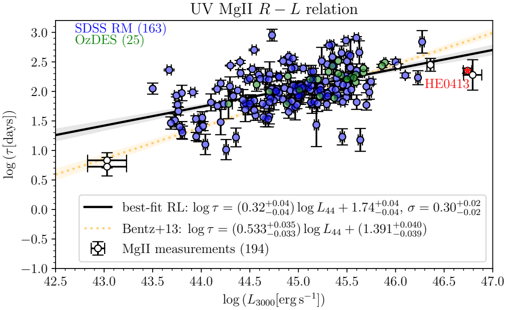


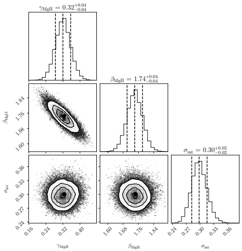

# Comparison of MgII and FeII R-L relations

- first UV FeII R-L relation presented in Prince+(2022)
- in Prince+(2023) we compare UV FeII with optical FeII and with MgII and H$\beta$ R-L relations
- signs of stratification (UV FeII closer to the SMBH than optical FeII emission)
- **MgII R-L relation is significantly flatter than the other relations**

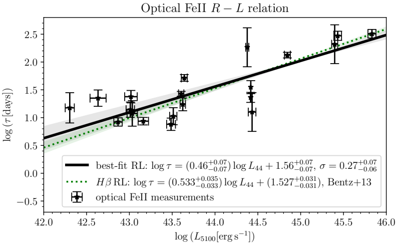


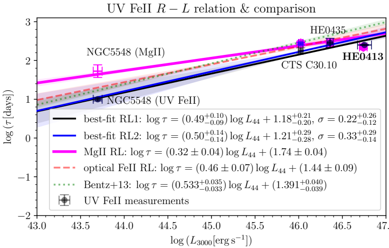

# CIV Radius-luminosity relation (towards high redshift)

First constrained HIL radius-luminosity relation, $0.001064 \leq z \leq 3.368$, 38 sources were collected and analyzed by Kaspi et al. (2021).

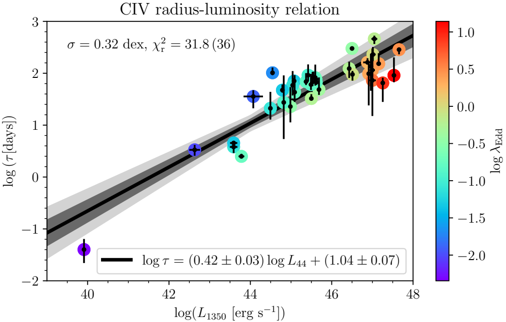


Taken from Cao, Zajaček et al. (2022)

# Datasets

Below we list **RM QSO data used for simultaneously constraining R-L relation as well as cosmological model parameters**. A better established BAO+$H(z)$ combined sample was used as a comparison sample.

| Sample | Source number | Redshift range | Reference |
|---|---|---|---|
| H$\beta$ RM QSOs | 118 | $0.0023 \leq z \leq 0.89$ | Khadka+22 |
| MgII RM QSOs | 69/78 | $0.0033 \leq z \leq 1.89$ | Khadka+21 |
| CIV RM QSOs | 38 | $0.001064 \leq z \leq 3.368$ | Cao+22 |
| BAO | 12 | $0.122 \leq z \leq 2.334$ | Cao & Ratra 2022 |
| $H(z)$ | 32 | $0.07 \leq z \leq 1.965$ | |

Table: Overview of used RM QSO data and the BAO+$H(z)$ comparison sample. BAO+H($z$) data are adopted from Tables 1 and 2 in Cao & Ratra 2022, MNRAS, vol. 513, p. 5686-5700.

# RM QSOs as standardizable candels

1. Perform reverberation mapping $\rightarrow$ continuum−broad line time lag $\tau_{\rm obs}$
2. Use radius−luminosity (R-L) relation to calculate theoretical time lags $\tau_{\rm th}$

$$\log\left(\frac{\tau_{\rm th}}{\rm day}\right) = \beta + \gamma \log\left[\frac{L_{\rm mon}(z,\mathbf{p})}{10^{44}\,{\rm erg\,s^{-1}}}\right],$$

   $L_{\rm mon} = 4\pi D_{\rm L}(z,\mathbf{p})^2\lambda F_{\lambda}$, where the luminosity distance is a function of the cosmological expansion rate $H(z,\mathbf{p})$, which depends on the considered cosmological model.
3. Maximize likelihood function to find simultaneously **R-L relation ($\beta$, $\gamma$) and cosmological model parameters p**

# RM QSOs as standardizable candels

3. Maximize likelihood function

$$lnLF = -\frac{1}{2}\sum_{i=1}^{N}\{\frac{[\log\tau_i^{\rm obs} - \log\tau_i^{\rm th}]^2}{s_i^2} + ln(2\pi s_i^2)\}$$

$$s_i^2 = \sigma^2_{\log\tau_{\rm obs,i}} + \gamma^2\sigma^2_{\log F_{3000,i}} + \sigma^2_{\rm int}$$

- 6 cosmological models: flat and non-flat ΛCDM, XCDM, and $\phi$CDM

  $H(z) = H_0\sqrt{\Omega_{m0}(1+z)^3 + \Omega_{k0}(1+z)^2 + \Omega_{\rm DE}(z)}$,
  For ΛCDM and XCDM: $\Omega_{\rm DE}(z) = \Omega_{\rm DE0}(1+z)^{1+\omega_{\rm X}}$
  $\phi$CDM (Peebles & Ratra 1988, Ratra & Peebles 1988):
  $V(\phi) = \frac{1}{2}\kappa m_{\rm p}^2\phi^{-\alpha}$ represents scalar field potential energy density
  $\Omega_{\rm DE} = \Omega_\phi(z,\alpha) = \frac{8\pi\rho_\phi}{32 m_{\rm p}^2 H_0^2}$

# Constraints from MgII sample

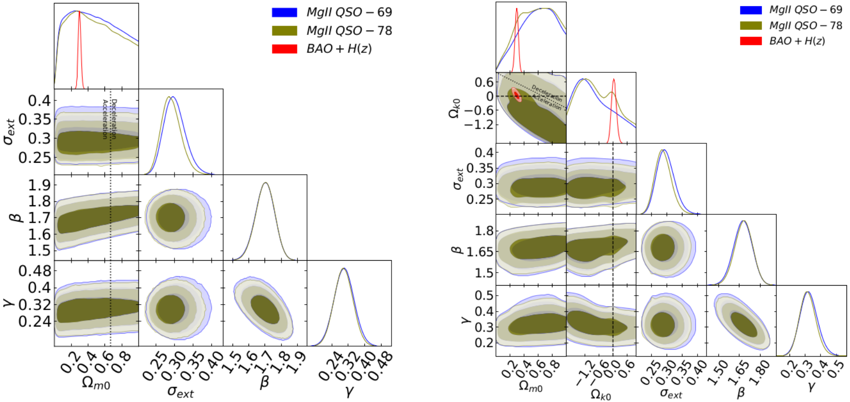


Likelihood distributions and contours for **flat (left)** and **non-flat (right)** ΛCDM model (see Khadka, Yu, Zajaček et al. 2021).

# Constraints from MgII+CIV+BAO+H(z) sample

## Consistent with BAO+H(z) – exemplary likelihood distributions for non-flat ΛCDM

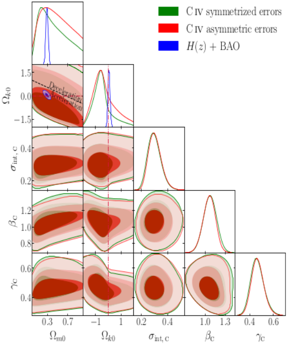


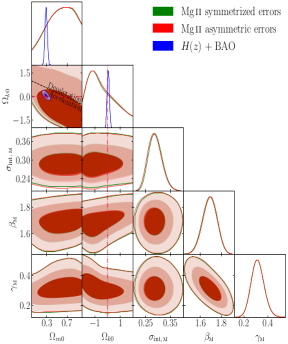


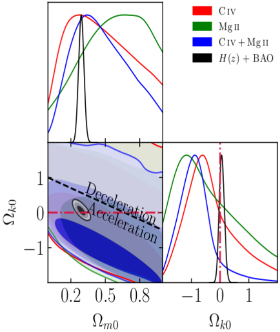


CIV and MgII quasars and their combination (Cao, Zajaček et al. 2022)

# Constraints from MgII+CIV+BAO+H(z) sample

## Consistent with BAO+H(z) – exemplary likelihood distributions for non-flat ΛCDM

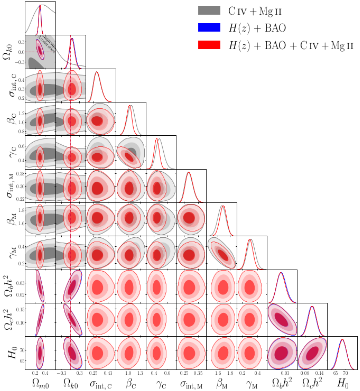


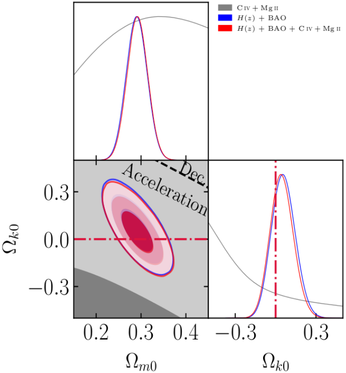


CIV and MgII quasars analyzed jointly with BAO+H(z) (Cao, Zajaček et al. 2022) $\rightarrow$ **quasars slightly tighten the constraints** ($\sim 0.1\sigma$ at most)

# H$\beta$ sample

- lower-redshift sample
- constraints in $\sim 2\sigma$ tension with BAO$+H(z)$ (**preference for decelerated expansion**)

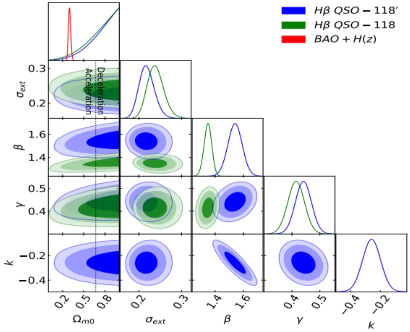


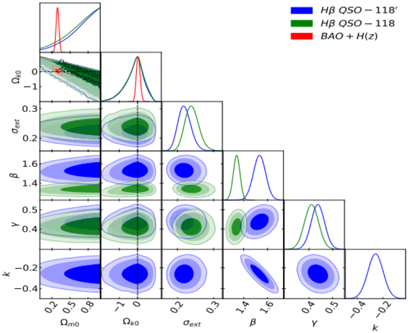


Likelihood contours for **flat (left)** and **non-flat (right)** ΛCDM model (see Khadka, Martinez-Aldama, Zajaček et al. 2022).

# Putting it all together

- Hubble diagram combining H$\beta$, MgII, and CIV RM QSOs with the maximum-likelihood flat ΛCDM model.

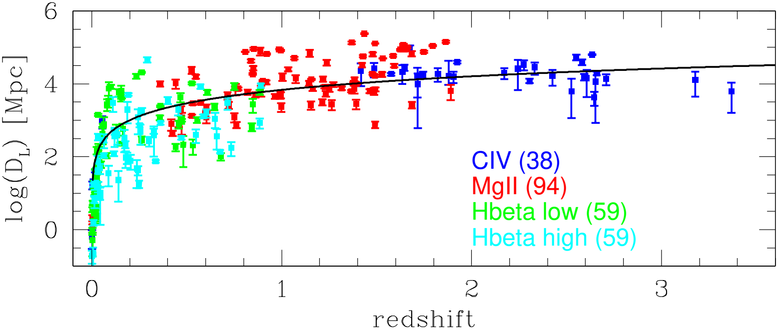


Figure: Hubble diagram of RM quasars (H$\beta$, MgII, and CIV) with the black solid line showing the inferred flat ΛCDM model with $H_0 = 68.86\,\mathrm{km\,s^{-1}\,Mpc^{-1}}$ and $\Omega_{\rm m0} = 0.295$.

# $R-L$ vs. $L_X - L_{UV}$ relation

- a sample of 58 X-ray detected reverberation-mapped quasars
- systematic differences between the two relations
- $L_X - L_{UV}$ shows preference for high $\Omega_{m0}$

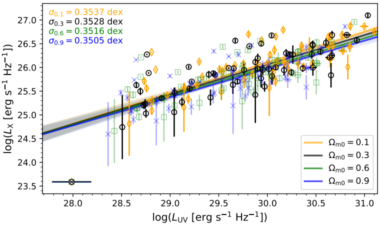


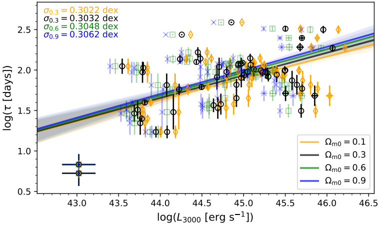


Left: $L_X - L_{UV}$ relation; Right: $R - L$ relation (Khadka, Zajaček et al., 2023)

# $R - L$ vs. $L_X - L_{UV}$ relation

- a sample of 58 X-ray detected reverberation-mapped quasars
- systematic differences between the two relations
- $L_X - L_{UV}$ shows preference for high $\Omega_{m0}$

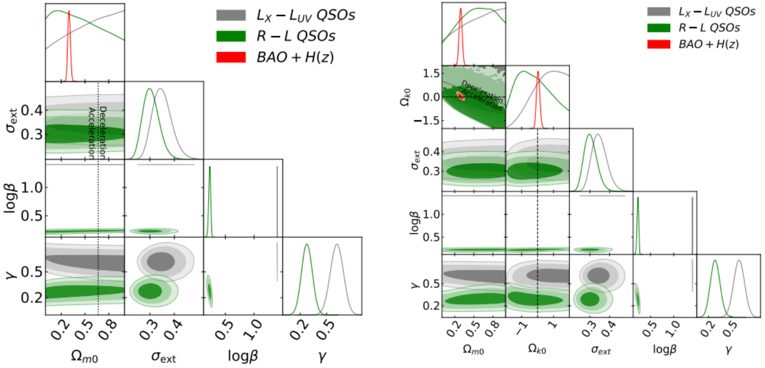


Likelihood distributions for ΛCDM (Khadka, Zajaček et al., MNRAS, 2023)

# $R - L$ vs. $L_X - L_{UV}$ relation

- normally, both relations should give the same luminosity distance to the same source
- however, we obtain **non-zero median and peak values** of luminosity distance difference distributions $\Delta \log D_{\rm L} = \log D_{L,L_X - L_{UV}} - \log D_{L,R-L}$, - systematically positive

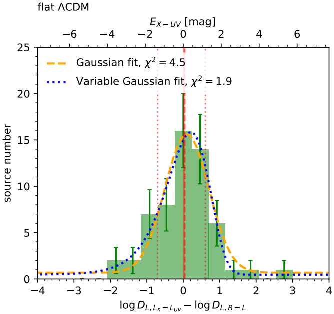


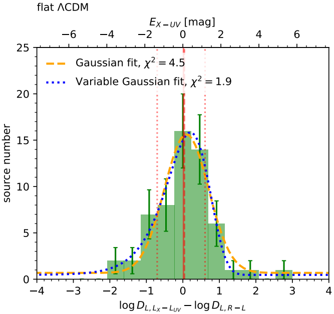


**Simple formula for UV/X-ray colour index:**

$E_{X-UV} = 5.001(1-\gamma') < (\Delta \log D_{\rm L})_{\rm ext} >$; **see Zajaček et al. (2024)**

# $R - L$ vs. $L_X - L_{UV}$ relation

- positively shifted peak and asymmetric distributions of $\Delta \log D_{\rm L}$ for all 6 cosmological models

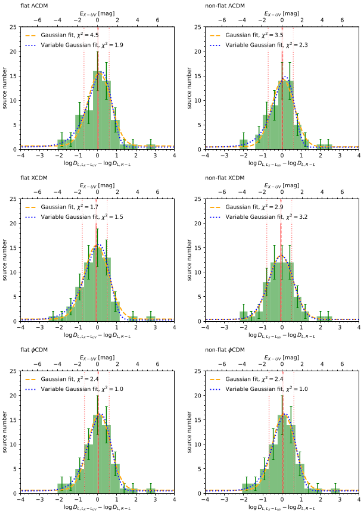

# $R - L$ vs. $L_X - L_{UV}$ relation

- consistent with dust-gas extinction of UV/X-ray light

$$
\begin{aligned}
&\Delta \log D_L \\
&= \underbrace{\overbrace{\frac{\beta' - \gamma'\eta'}{2(1-\gamma')} + \frac{\beta - \log\tau}{2\gamma} - \frac{\eta}{2} + 7.518}^{\delta} + \frac{\log F_{\rm UV,\,int} - \log F_{\rm X,ir}}{2(1-\gamma')}}_{=0 \text{ for intrinsic quasar emission}} \\
&+ \underbrace{\frac{(\tau_X - \tau_{\rm UV})\log e}{2(1-\gamma')}}_{\text{extinction contribution}},
\end{aligned}
$$

# Conclusions

We showed that **broad-line region radius-luminosity relation** is independent of a cosmology model, and thus **can be applied to standardize RM quasars.** The main conclusions can be summarized as follows

- cosmological constraints from reverberation-mapped quasars are weaker in comparison with BAO+H(z) data so far, though there is a prospect of tightening the constraints thanks to future quasar monitoring, such as using Vera C. Rubin observatory performing the *Legacy Survey of Space and Time – LSST*,
- for MgII and CIV quasars, constraints are consistent with BAO+H(z) (Khadka et al. 2021, Cao et al. 2022). However, for H$\beta$ quasars, there is $\sim 2\sigma$ tension with BAO+H(z) constraints (Khadka et al. 2022),
- the joint analysis MgII+CIV+BAO+H(z) leads to mildly tighter cosmological constraints (at most $\sim 0.1\sigma$) in comparison with BAO$+H(z)$ sample alone (Cao et al. 2022).

# Conclusions

Recent paper on the effect of (dust) extinction on measuring luminosity distances of quasars arXiv: 2305.08179

The Astrophysical Journal, 961:229 (18pp), 2024 February 1 https://doi.org/10.3847/1538-4357/ad11dc


## Effect of Extinction on Quasar Luminosity Distances Determined from UV and X-Ray Flux Measurements

Michal Zajaček[1], Bożena Czerny[2], Narayan Khadka[3,4], Mary Loli Martínez-Aldama[5,6], Raj Prince[2], Swayamtrupta Panda[7,9], and Bharat Ratra[8]

[1] Department of Theoretical Physics and Astrophysics, Faculty of Science, Masaryk University, Kotlářská 2, 611 37 Brno, Czech Republic; zajacek@physics.muni.cz
[2] Center for Theoretical Physics, Polish Academy of Sciences, Al. Lotników 32/46, 02-668 Warsaw, Poland
[3] Department of Physics, Bellarmine University, 2001 Newburg Rd, Louisville, KY 40205, USA
[4] Department of Physics and Astronomy, Stony Brook University, Stony Brook, NY 11794, USA
[5] Astronomy Department, Universidad de Concepción, Casilla 160-C, Concepción 4030000, Chile
[6] Instituto de Física y Astronomía, Facultad de Ciencias, Universidad de Valparaíso, Gran Bretaña 1111, Playa Ancha, Valparaíso, Chile
[7] Laboratório Nacional de Astrofísica—MCTI, R. dos Estados Unidos, 154—Nações, Itajubá—MG, 37504-364, Brazil
[8] Department of Physics, Kansas State University, 116 Cardwell Hall, Manhattan, KS 66506, USA

*Received 2023 August 23; revised 2023 November 16; accepted 2023 December 2; published 2024 January 31*

### Abstract

In Khadka et al., a sample of X-ray-detected reverberation-mapped quasars was presented and applied for the comparison of cosmological constraints inferred using two well-established relations in active galactic nuclei—the X-ray/UV luminosity ($L_X$–$L_{\rm UV}$) relation and the broad-line region radius–luminosity ($R$–$L$) relation. $L_X$–$L_{\rm UV}$ and $R$–$L$ luminosity distances to the same quasars exhibit a distribution of their differences that is generally asymmetric and positively shifted for the six cosmological models we consider. We demonstrate that this behavior can be interpreted qualitatively as arising as a result of the dust extinction of UV/X-ray quasar emission. We show that the extinction always contributes to the nonzero difference between $L_X$–$L_{\rm UV}$-based and $R$–$L$-based luminosity distances and we derive a linear relationship between the X-ray/UV color index $E_{X-{\rm UV}}$ and the luminosity-distance difference, which also depends on the value of the $L_X$–$L_{\rm UV}$ relation slope. Taking into account the median and the peak values of the luminosity-distance difference distributions, the average X-ray/UV color index falls in the range of $\overline{E}_{X-{\rm UV}} = 0.03$–$0.28$ mag for the current sample of 58 sources. This amount of extinction is typical for the majority of quasars and can be attributed to the circumnuclear and interstellar media of host galaxies. After applying the standard hard X-ray and far-UV extinction cuts, heavily extincted sources are removed but overall the shift toward positive values persists. The effect of extinction on luminosity distances is more pronounced for the $L_X$–$L_{\rm UV}$ relation since the extinction of UV and X-ray emissions both contribute.

*Unified Astronomy Thesaurus concepts:* Cosmology (343); Cosmological parameters (339); Observational cosmology (1146); Active galaxies (17); Quasars (1319); Interstellar dust extinction (837)

# Conclusions

Popular version on https://phys.org/news/2024-02-galaxies-standard-candles-culprit-discrepanc html

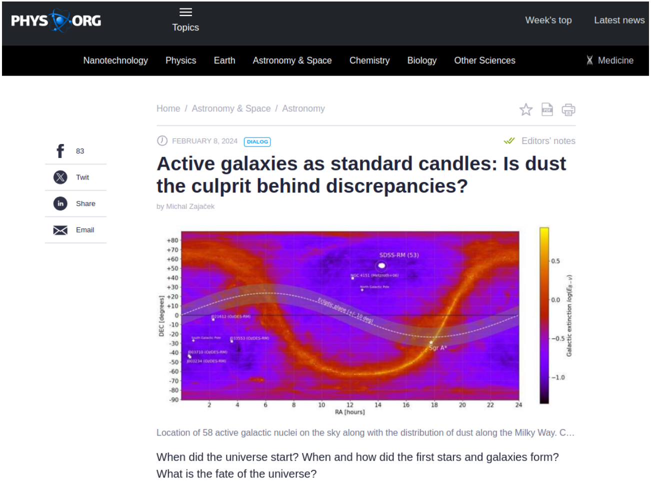

PHYS ORG | Topics | Week's top | Latest news

Nanotechnology | Physics | Earth | Astronomy & Space | Chemistry | Biology | Other Sciences | Medicine

Home / Astronomy & Space / Astronomy

FEBRUARY 8, 2024 DIALOG | Editors' notes

83 | Twit | Share | Email

## Active galaxies as standard candles: Is dust the culprit behind discrepancies?

by Michal Zajaček

Location of 58 active galactic nuclei on the sky along with the distribution of dust along the Milky Way. C…

When did the universe start? When and how did the first stars and galaxies form? What is the fate of the universe?

# Conclusions

Summary paper published in Astronomy and Space Science arXiv: 2209.06563

Astrophysics and Space Science (2023) 368:8
https://doi.org/10.1007/s10509-023-04165-7

RESEARCH

## Accretion disks, quasars and cosmology: meandering towards understanding

**Bożena Czerny[1] · Shulei Cao[2] · Vikram Kumar Jaiswal[1] · Vladimír Karas[3] · Narayan Khadka[4] · Mary Loli Martínez-Aldama[5] · Mohammad Hassan Naddaf[1] · Swayamtrupta Panda[6] · Francisco Pozo Nuñez[7] · Raj Prince[1] · Bharat Ratra[2] · Marzena Sniegowska[8,1] · Zhefu Yu[9] · Michal Zajaček[10]**

Received: 14 September 2022 / Accepted: 30 January 2023 / Published online: 8 February 2023


**Abstract**
As Setti and Woltjer noted back in 1973, one can use quasars to construct the Hubble diagram; however, the actual application of the idea was not that straightforward. It took years to implement the proposition successfully. Most ways to employ quasars for cosmology now require an advanced understanding of their structure, step by step. We briefly review this progress, with unavoidable personal biases, and concentrate on bright unobscured sources. We will mention the problem of the gas flow

# Galactic Nuclei in the Cosmological context 2024


https://gnc2024.physics.muni.cz/

MASARYK
UNIVERSITY